Extended Depth-of-Field Projector by Fast Focal Sweep Projection

Daisuke Iwai, Shoichiro Mihara, and Kosuke Sato, *Member, IEEE*

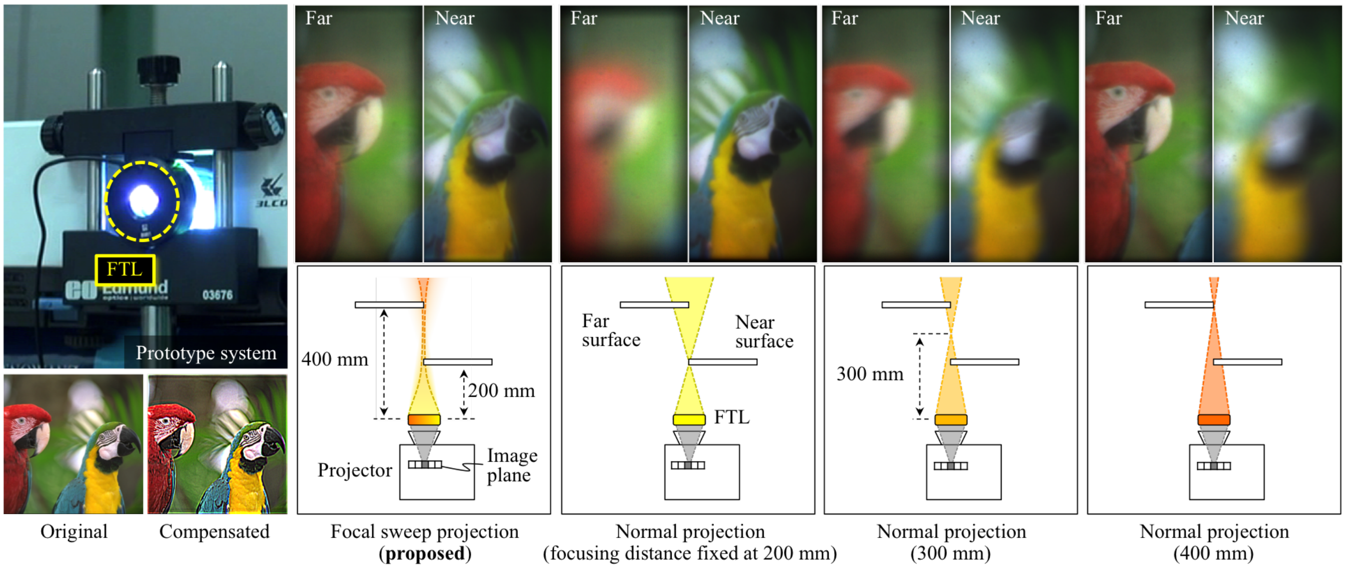

Fig. 1. Extending projector depth-of-field (DOF) by fast focal sweep projection on projection surfaces with different depths: (top-left) proposed extended DOF projector is achieved by placing an electrical focus tunable lens (FTL) before the projector's objective; (bottom-left) original projection image for normal projection is compensated for IPSF to generate a projection image for the proposed focal sweep projection; (top-right) projected results on two planar surfaces placed at depths of 200 and 400 mm from the FTL; (bottom-right) system configurations.

Abstract— A simple and cost-efficient method for extending a projector's depth-of-field (DOF) is proposed. By leveraging liquid lens technology, we can periodically modulate the focal length of a projector at a frequency that is higher than the critical flicker fusion (CFF) frequency. Fast periodic focal length modulation results in forward and backward sweeping of focusing distance. Fast focal sweep projection makes the point spread function (PSF) of each projected pixel integrated over a sweep period (IPSF; integrated PSF) nearly invariant to the distance from the projector to the projection surface as long as it is positioned within sweep range. This modulation is not perceivable by human observers. Once we compensate projection images for the IPSF, the projected results can be focused at any point within the range. Consequently, the proposed method requires only a single offline PSF measurement; thus, it is an open-loop process. We have proved the approximate invariance of the projector's IPSF both numerically and experimentally. Through experiments using a prototype system, we have confirmed that the image quality of the proposed method is superior to that of normal projection with fixed focal length. In addition, we demonstrate that a structured light pattern projection technique using the proposed method can measure the shape of an object with large depth variances more accurately than normal projection techniques.

Index Terms—Projection display, extended depth-of-field projector, focal sweep, immersive virtual reality, spatial augmented reality

1 Introduction

The application of projection display technology is expanding from indoor immersive virtual reality (VR) systems with concave or curved surfaces to outdoor projection mapping that provides mixed reality experiences on the surfaces of large buildings. Spatial augmented reality (AR) is an active field in projection display research, in which arbitrarily shaped objects are visually augmented by superimposing graphics from projectors [7]. For example, a user can interactively paint a product mockup using a tracked pen device, on which the painted result is projected [2]. Projector-camera systems (ProCams) have also been widely used in the shape measurement of various objects, such as historical artifacts and the human body, for virtualizing real world. In such applications, images are projected on nonplanar surfaces that sometimes have large depth variances.

Projectors are inherently designed with a large aperture to minimize the loss of light emitted from a light source. However, this optical design leads to a significantly narrow depth-of-field (DOF). Consequently, an image projected on a surface with large depth variance can become blurred easily. Previous study has attempted to address this defocus issue by applying image pre-correction techniques, such as the Wiener filter, to sharpen projected results [8]. However, such techniques are closed-loop processes, i.e., they require the measurement of the point spread function (PSF) for each projected pixel on the projection surface before correcting projection images, which must occur whenever the PSF is changed by the movement of either the projector or the surface. The PSF, which varies as per the distance from the

- *Daisuke Iwai is with Osaka University. E-mail: daisuke.iwai@sys.es.osaka-u.ac.jp.*
- *Shoichiro Mihara is with Osaka University. E-mail: mihara@sens.sys.es.osaka-u.ac.jp.*
- *Kosuke Sato is with Osaka University. E-mail: sato@sys.es.osaka-u.ac.jp.*

Manuscript received 18 Sept. 2014; accepted 10 Jan. 2015. Date of Publication 20 Jan. 2015; date of current version 23 Mar. 2015. For information on obtaining reprints of this article, please send e-mail to: reprints@ieee.org.

projector to a projection surface, is generally measured by projecting structured light patterns (e.g., a dot pattern) on the surface and capturing the projected results with a camera. Therefore, a pre-correction approach is not suitable for projecting a sharp image on a moving object because the PSF changes over time as per the object's movement; thus, it must be measured with distracting artificial pattern projections for nearly every frame.

We propose an open-loop approach to extend a projector's DOF. The proposed method requires only a single offline PSF measurement. The proposed approach is simple and cost-efficient. We leverage liquid lens technology, which enables periodic modulation of the focal length of a projector at a frequency that is higher than the critical flicker fusion (CFF) frequency. Fast periodic focal length modulation results in forward and backward sweeping of the focal distance of the projected image. Such fast focal sweep projection makes the PSF of each projected pixel integrated over a sweep period (i.e., integrated PSF; IPSF) nearly invariant to the distance from the projector to the surface as long as it is within the sweep range. This modulation is not perceivable by human observers. Several computational photography studies have examined the focal sweep technique to extend a camera's DOF by utilizing IPSF's invariance on the camera's image plane [13]. However, the IPSF of a focal sweep projector must be considered for a projection surface with depth variance rather than for the projector's image plane. We verify the approximate invariance of the projector's IPSF both numerically and experimentally. Through experiments using a prototype system, we evaluate how the proposed method, compared to normal projection with a fixed focal length, improves projected image qualities on various surface shapes and moving objects (Fig. 1). We also demonstrate how accurately a structured light pattern projection technique combined with the proposed method can measure the shape of an object with large depth variance compared to normal projection. To the best of our knowledge, this is the first attempt to achieve extended projector DOF by applying focal sweep.

To summarize, we provide the following contributions:

- We realize an extended DOF projector by applying a fast focal sweep technique.
- We numerically and experimentally confirm that the projector's IPSF on the projection surface is nearly invariant to the distance from the projector to the surface.
- We confirm that the proposed method improves the projected image quality on moving or static surfaces with large depth variances compared to normal projection with fixed focal length.
- We demonstrate that the proposed method increases the accuracy of shape measurement in active stereo method using structured light pattern projection.

2 Related Study

The proposed method is strongly related to two existing research topics: extended DOF projectors (Section 2.1) and focal sweep cameras (Section 2.2). Here, we describe previous study and state our contributions (Section 2.3).

2.1 Extended DOF Projection

Previous extended DOF projection techniques fall into two categories: single-projector and multiple-projector approaches. These techniques have primarily been proposed in ProCam research [6].

Single-projector approaches digitally sharpen original images before projection so that an optically defocused projection closely approximates the original (i.e., unblurred) image. Defocus blur of a projected image is explained mathematically as the convolution of a PSF and the original image. If the PSF of a projector on an object's surface is estimated correctly, a defocus-free image can be displayed by digitally correcting the original image using a deconvolution method, such as the Wiener filter [8]. Zhang and Nayar formulated image correction as a constrained optimization problem [25]. Grosse et al. proposed the insertion of a coded aperture to decrease the loss of high frequency components in the image correction process [9]. These studies estimated PSFs by projecting pattern images (e.g., two-dimensional array of dots or crosses) and capturing the displayed results in advance.

Bimber and Emmerling applied multiple projectors, each with a focal plane at a unique distance, to realize multifocal projection [5]. For each point on a projection surface, they selected an optimal projector that could display the finest image on the point. Their multi-projector approach does not require deconvolution; however, when an object moves, it does require the projection of spatial pattern images on the surface to estimate PSFs from every projector. Nagase et al. proposed a model-based multi-projector method that selects the optimal projector by estimating PSFs from geometric information, such as the shape of a projection surface and the relative position and the pose of the surface to projectors [19]. Although this method does not need to project spatial pattern images for PSF measurement, measuring the geometric information of the target surface is required for each frame.

The above-mentioned methods apply closed-loop solutions that require either measurement or the estimation of PSFs at the current frame for the next frame's image correction. Therefore, projected results cannot be optimized for the current frame when a projection surface moves. The optimization for the current frame is achieved only when the movement of a projection surface is known and the PSF measurement or estimation for the surface is performed in advance, as proposed in [3].

2.2 Focal Sweep Camera

Imaging systems often require very large DOFs in particular application fields, such as microscopy and surveillance. Although the DOF of such systems can be increased by narrowing the aperture, this leads to significant reduction of the signal-to-noise ratio (SNR) of the captured images. A focal sweep technique has been researched to extend the DOF of an imaging system while maintaining high SNR.

The focal sweep principle was originally proposed by Häusler, who extended the DOF of microscopes [10]. In that pioneering work, a microscopic object was moved along the optical axis while capturing, and the captured image was then deconvolved using IPSF, which was proved constant over the moving range, to acquire a deblurred image of the specimen. Liu and Hua proposed another approach that moved the focal length rather than the microscopic object to extend the DOF of microscopes [14]. A different but similar method is the confocal imaging technique. This technique sweeps two confocal pinholes simultaneously, one for illumination and the one for observation (camera), over a particular depth range [17]. Because both illumination and observation are focused, clear cross-sectional views can be acquired.

Recently, the focal sweep principle was extended to conventional photography that captures larger depth ranges. Kuthirummal et al. proposed to apply a focal sweep technique to extend the DOF of a conventional camera. They showed various possible applications, such as tilted DOF, nonplanar DOF, and DOF manipulation [13, 18]. Extended DOF video has also been realized by applying high-frequency periodic focal sweep [15].

Although focal sweep techniques for imaging systems have been researched intensively, focal sweep techniques for projectors have not been well investigated. With increasing demand for image projection on surfaces with large depth variances, it is becoming increasingly important to realize an extended DOF projector while maintaining maximum luminance.

2.3 Proposed Method

We propose a single-projector approach to extend a projector's DOF. We apply a fast focal sweep technique to a projector and numerically and empirically investigate the invariance of IPSFs on projection surfaces with large depth variances. We demonstrate that the proposed method is an open-loop process and can extend a projector's DOF using only a single offline PSF measurement. We also demonstrate that the projected results are always in focus when the projection surface has large depth variance and when it moves.

One might think that the DOF issue can be solved more easily by simply replacing existing lens-based projectors with laser projectors

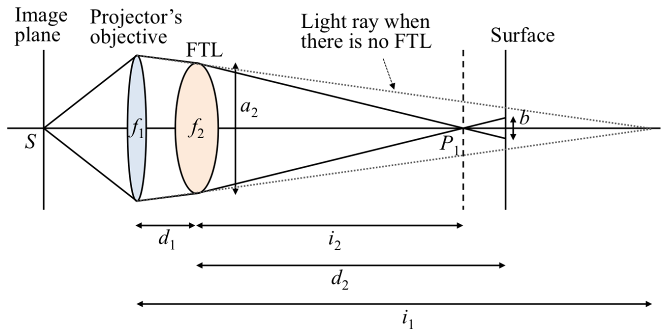

Fig. 2. Optical model of focal sweep projection.

that do not suffer defocus blur [1]. However, laser projectors suffer from other inherent technical issues, such as speckle noise and eye safety, which have not yet been solved. Therefore, a lens-based projector is a better option than a laser projector for many applications, particularly those that require high-quality and bright image projection. Our simple and cost-efficient method for extending a lens-based projector's DOF can contribute to such applications by providing all-in-focus projection.

3 Fast Focal Sweep Projection

Here, we describe our focal sweep projection principle to extend the DOF of a projector. First, we explain how a projected image sequence from a focal sweep projector is integrated in the human visual system (HVS) (Section 3.1). The computational model of projector IPSF is then derived (Section 3.2). We then numerically evaluate how the IPSF is invariant to scene depths (Section 3.3). Finally, we describe a technique to extend the DOF of a focal sweep projector by leveraging the approximate depth invariance of the IPSF (Section 3.4).

3.1 Fast and Linear Focal Length Modulation

Humans do not perceive flicker when light sources are turned on and off at frequencies higher than 60 Hz, which is generally referred to as CFF frequency [12]. The HVS integrates visual stimuli presented within 16-20 ms. Therefore, when the focal length of a projector lens is periodically modulated at CFF frequency or higher, the observer perceives the integration of projected images that are periodically sharpened and blurred on a projection surface.

We assume that the focal length of a projector is modulated so that the diameter of a blur circle is periodically modulated at a uniform speed. Previous computational photography research has applied such linear modulation and has proved that this makes the IPSF on a camera's image plane identical regardless of the distance from the camera to the captured scene [13, 15]. The recent development of electrical focus tunable lenses (FTL) based on optical fluids allows us to realize such modulation [20].

3.2 Computational Model of Projector IPSF

In this section, we describe an IPSF computational model for a pixel projected by a projection system wherein an FTL is placed before the projector's objective, as shown in Fig. 2. A pixel projected from a point S on the image plane of the projector is refracted at the projector's objective (focal length: f_1), and then at the FTL (focal length: f_2). The projected pixel is then focused at P_1, which is the image point of the compound lens.

Here, a_2, d_2, and i_2 are the diameter of the FTL's circular aperture, the distance from the FTL's principal point to a projection surface, and the distance from the principal point to the image point (i.e., focusing distance), respectively. The diameter of the blur circle b on the projection surface can be computed using geometrical similarity as follows:

$$b = \left| \frac{a_2 d_2}{i_2} - a_2 \right|. \tag{1}$$

The pixel at point S is not an ideal point light source; therefore, the PSF of the projected pixel cannot be represented as a pillbox function but is generally approximated as the following Gaussian function:

$$PSF(r,b) = \frac{2}{\pi b^2} \exp\left(-\frac{2r^2}{b^2}\right), \tag{2}$$

where r is the distance from the center of the blur circle. Here, d_1 and i_1 are the distance between the principal points of the projector's objective and FTL and the focusing distance of the projector's objective, respectively. Thus, the thin lens equation represents the following relationship:

$$\frac{1}{i_2} = \frac{1}{f_2} + \frac{1}{i_1 - d_1}. \tag{3}$$

Considering periodical modulation, we must consider cases wherein the diameter of the blur circle decreases and increases linearly. Each PSF consists only of positive values; therefore, the integration of PSFs results in the same value for both cases. Here, we only consider the linearly decreasing case. We apply the following equation for the focal length $f_2(t)$ of the FTL so that the diameter of the blur circle $b(t)$ is modulated at a uniform speed.

$$f_2(t) = \frac{1}{\alpha t + \beta}, \quad (\alpha > 0,\ \beta > 0), \tag{4}$$

where α and β are the coefficients of the monotonically decreasing function.

We can periodically modulate the diameter of the blur circle $b(t)$ by modulating the FTL's focal length $f_2(t)$, resulting in forward and backward modulation of focusing distance $i_2(t)$. When $b(t)$ is modulated at a frequency ν of CFF frequency or higher, the observer perceives the integration of the PSFs; i.e., IPSFs. Therefore, the perceived IPSF can be represented as follows:

$$IPSF(r) = \int_0^T PSF(r, b(t))dt, \tag{5}$$

where the focal length $f_2(t)$ decreases from $t = 0$ to T. T represents the half of a period, thus $T = \frac{1}{2\nu}$. In principle, focusing distance $i_2(t)$ is shortest when the focal length $f_2(t)$ takes the minimum value, while it is longest when $f_2(t)$ takes the maximum value. We refer to the range between the shortest and longest focusing distances as the "sweep range". We assume that the projection surface is either located or moved within the sweep range. In this case, $b(t)$ becomes discontinuous at t_f when the image point corresponds to the surface position (i.e., $i_2(t_f) = d_2$). Therefore, we reformulate the IPSF computation (Eq. 5) by dividing it at t_f as follows:

$$IPSF(r) = \int_0^{t_f} PSF(r, b(t))dt + \int_{t_f}^{T} PSF(r, b(t))dt. \tag{6}$$

As mentioned above, we consider a case wherein the focal length $f_2(t)$, and consequently the focusing distance $i_2(t)$, decrease monotonically. Therefore, $i_2(t) \geq d_2$ when $0 \leq t \leq t_f$ and $i_2(t) < d_2$ when $t_f < t \leq T$. Thus, the calculation of $b(t)$ (Eq. 1) can be rewritten as follows:

$$b(t) = \begin{cases} -\dfrac{a_2 d_2}{i_2(t)} + a_2, & (0 \leq t \leq t_f) \\[2ex] \dfrac{a_2 d_2}{i_2(t)} - a_2, & (t_f < t \leq T) \end{cases}. \tag{7}$$

From Eqs. 4, 7, and 3, the temporal differentiation of $b(t)$ can be computed as follows:

$$\frac{db(t)}{dt} = \begin{cases} -a_2 d_2 \alpha, & (0 \leq t \leq t_f) \\[1ex] a_2 d_2 \alpha, & (t_f < t \leq T) \end{cases}. \tag{8}$$

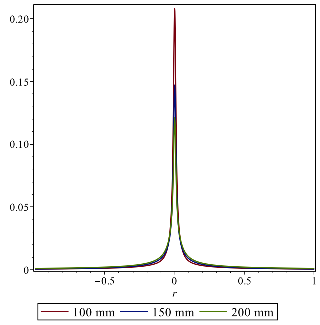

(a)

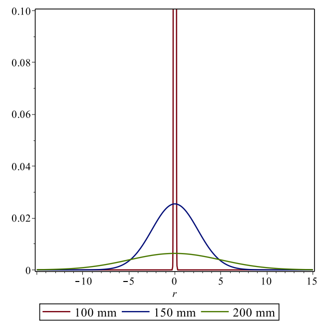

(b)

Fig. 3. IPSF simulation results at different scene depths: (a) focal sweep projection; (b) normal projection with fixed focusing distance.

By substituting the integration variables of Eq. 6 with Eq. 8, the IPSF computation can be rewritten as follows:

$$\begin{aligned} IPSF(r) \quad &= \quad -\frac{1}{a_2 d_2 \alpha}\int_{b(0)}^{b(t_f)} PSF(r, b(t))db \\ &\quad +\frac{1}{a_2 d_2 \alpha}\int_{b(t_f)}^{b(T)} PSF(r, b(t))db. \end{aligned} \tag{9}$$

Thus, we obtain

$$\begin{aligned} IPSF(r) \quad &= \quad -\frac{1}{a_2 d_2 \alpha \sqrt{2\pi} r}\left\{\mathrm{erf}\left(\frac{\sqrt{2}r}{b(0)}\right)\right. \\ &\quad \left. +\mathrm{erf}\left(\frac{\sqrt{2}r}{b(T)}\right) - 2\mathrm{erf}\left(\frac{\sqrt{2}r}{b(t_f)}\right)\right\}, \end{aligned} \tag{10}$$

by solving Eq. 9 using the Maple computer algebra system [24].

3.3 IPSF Simulation

Using the derived computational model, we simulated IPSFs for projection surfaces with different depths to evaluate how IPSFs are invariant to scene depths numerically. The simulation was performed assuming a projection system with an FTL placed before a normal projector. Here, $a_2 = 10$ mm, $i_1 = 3000$ mm, $d_1 = 5$ mm, and $\alpha = 0.575$.

Figure 3(a) shows the one-dimensional profile of an IPSF for three projection surfaces with depths (i.e., d_2) of 100-200 mm from the FTL. The FTL is modulated so that the focusing distance $i_2(t)$ is modulated periodically between 100 and 200 mm at 50 Hz. We simulated a half cycle of the modulation, in which the focal length $f_2(t)$, and consequently the focusing distance $i_2(t)$, decrease monotonically; i.e., $T = 0.01$, $100 \le i_2(t) \le 200$, $i_2(0) = 200$, and $i_2(T) = 100$. Figure 3(b) shows a PSF for the same projection surfaces, which was computed with a fixed focal length of the FTL so that the focusing distance was fixed at 150 mm; i.e., $i_2(t) = 150$ $(0 \le t \le T)$. The profiles shown in Fig. 3(a) appear similar, while those shown in Fig. 3(b) differ significantly. We confirmed that the IPSFs of focal sweep projection are nearly invariant to scene depths as long as the projection surface is located within the sweep range.

3.4 Extending Projector DOF

The IPSF of a focal sweep projector is nearly invariant to scene depth; i.e., the projected result is always blurred with the same blur kernel, which is the IPSF. Therefore, once a projection image is generated by applying a blur correction technique to an original projection image to compensate for the IPSF, the projected result is theoretically nearly in focus on a projection surface located at any depth within the sweep range.

Although the Wiener filter is generally used for blur compensation, it only works effectively when a PSF is spatially uniform across a projection image. Through a preliminary experiment, we determined that the IPSF varies spatially due to imperfections in the applied optics (Section 4.2). Therefore, we generate projection images by applying a blur compensation technique [25] that was developed to compensate for the defocus blur of a projected image with spatially varying PSFs based on an iterative, constrained, and steepest-descent algorithm.

Fig. 4. System overview.

4 Experiment

Using a prototype system, we conducted several experiments to validate the proposed method. We verified the linearity of focusing distance modulation, which ensures the IPSF invariance to scene depth (Section 4.1). The actual IPSFs were measured to determine the invariance (Section 4.2). We then conducted projection experiments to assess the displayed image quality with different projection surfaces, including a moving surface (Section 4.3). We demonstrate that the proposed method provides more accurate shape measurement results than normal projection in an active stereo application (Section 4.4).

4.1 Experimental Setup

We constructed the prototype system shown in Fig. 4. An FTL (Optotune, EL-10-30) was placed before the objective of the projector (Epson, EMP-1710). In the data sheet of the FTL, we determined the following relationship between input current I and focal length f_2

$$f_2(I) = \frac{1}{\alpha_I I + \beta_I}, \quad (\alpha_I > 0,\ \beta_I > 0). \tag{11}$$

From this relationship and Eq. 4, we decided to modulate current $I(t)$ using a triangle wave, which theoretically ensures the modulation of the diameter of blur circle $b(t)$ at a uniform speed. The modulation signal (digital) was sent from a PC. This signal was first converted to an analog signal, and then amplified before being sent to the lens. The input current of the triangle wave applied to the FTL was 86-137 mA, and the focusing distance $i_2(t)$ was modulated periodically from 200 to 400 mm. The frequency of the wave was set to 60 Hz.

We verified the linearity of the modulation using the prototype system. As shown in Fig. 5(a), we placed a photodiode (OSRAM Opto Semiconductors, SFH203P) within sweep range. A white dot was projected with the proposed focal length modulation in a dark room such that the center of the dot always illuminated the photodiode. The output voltage from the photodiode measured by an oscilloscope took the maximum value when the dot was focused at the photodiode. The output voltage decreased as the dot blurred. The photodiode measured the illuminance of the projected dot, which is inversely proportional to the area of the dot. Consequently, the square root of the illuminance is inversely proportional to the diameter of the dot (i.e., blur circle) $b(t)$. We acquired the illuminance value from measured voltage using the input/output characteristics from the photodiode specification

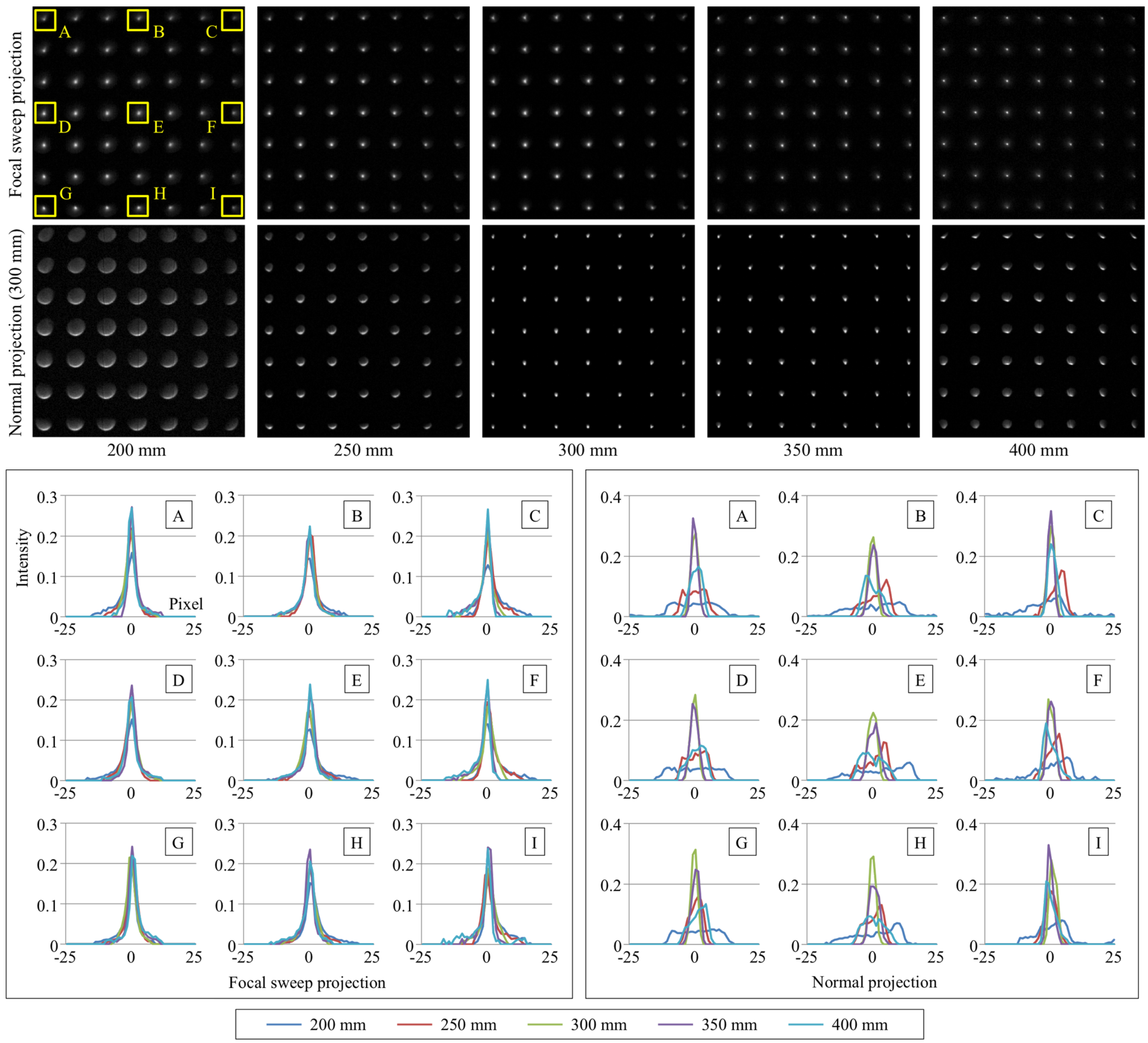

Fig. 6. PSF measurement: (top) measured dot patterns with scene depths of 200 to 400 mm; (bottom) one-dimensional profiles of measured PSFs at nine selected locations (A-I).

sheet. We then computed the reciprocal of the square root of the acquired illuminance to calculate the diameter of the dot. Note that the calculated diameter is not identical with an actual value; it is a relative value that includes a proportionality constant. The relative value was sufficient for this experiment, i.e., linearity verification. Figure 5(b) shows the time series of the input current values to the FTL and the computed relative diameters. As can be seen in Fig. 5(b), the relative diameter was nearly a triangle wave with the same frequency of the input wave (60 Hz). Therefore, we confirmed that the diameter of the blur circle $b(t)$ was modulated at a uniform speed.

Note that we used the central square region (300×300 pixels) of the projector in the following experiments. The other peripheral region could not be used due to a vignetting effect caused by the smaller aperture of the FTL than the projector objective.

4.2 Empirical Evaluation of IPSF

We evaluated the approximate invariance of the projector's IPSF experimentally. A 7×7 dot pattern with horizontal and vertical intervals of 50 pixels, covering 300×300 pixels in a projection image, was projected on a planar surface at five different depths (i.e., 200, 250, 300, 350, and 400 mm) from the FTL. The evaluation was performed using two projection systems, i.e., focal sweep projection, where the FTL was modulated with the parameters described in Section 4.1, and normal projection, where the FTL was not modulated and focusing distance was fixed at 300 mm from the FTL.

We captured the projected pattern using a camera (Canon EOS Digital Rebel XTi) at a shutter speed of 1/60 s. Figure 6 shows the captured images and the one-dimensional profiles of the captured IPSFs of nine dots located at the center, sides, and the corners of the projected patterns. From the results, we confirmed that the IPSFs of the focal sweep projection were nearly invariant to the depths, while those of the normal projection differed significantly according to the depths.

As described in Section 3.4, we applied a blur compensation method [25] that can deal with spatially varying PSFs. The method requires the IPSFs of all projector pixels. Thus, we derived the IPSFs of the other pixels from the 7×7 IPSFs at depths of 300 mm by applying spline interpolation.

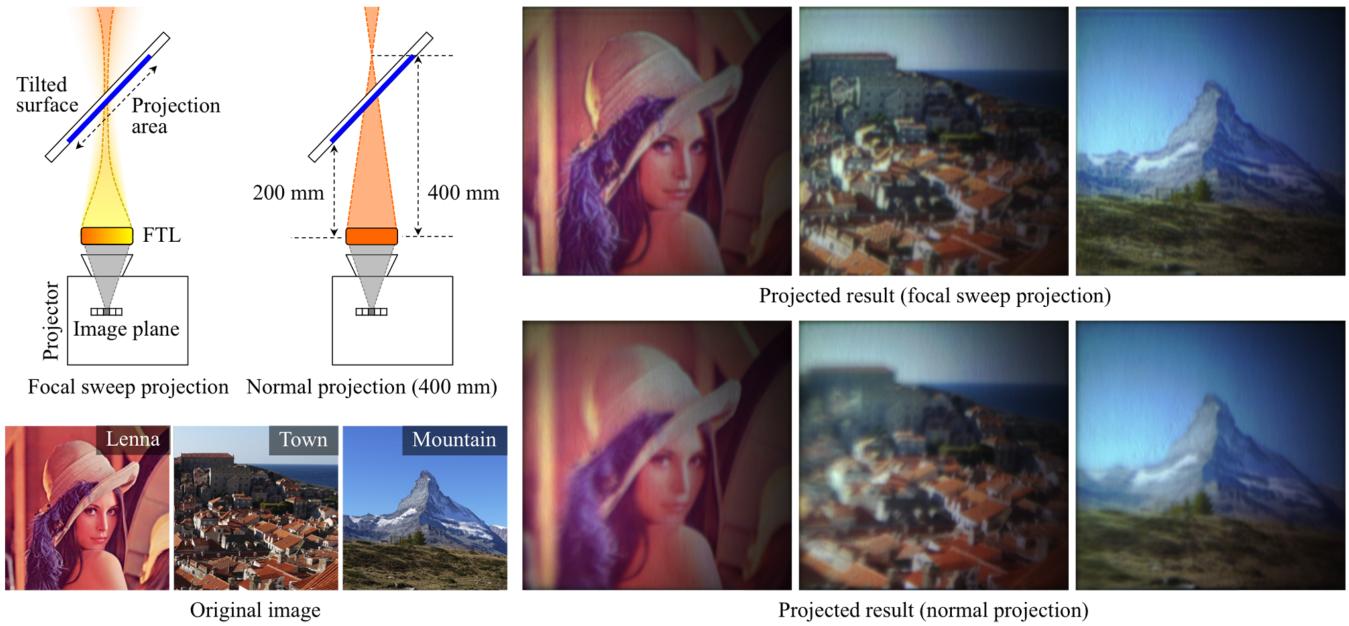

Fig. 7. Extended DOF projector demonstration with tilted projection surface: (top-left) comparison of proposed focal sweep projection and normal projection (fixed focusing distance, 400 mm); (bottom-left) three original projection images; (right) projected results.

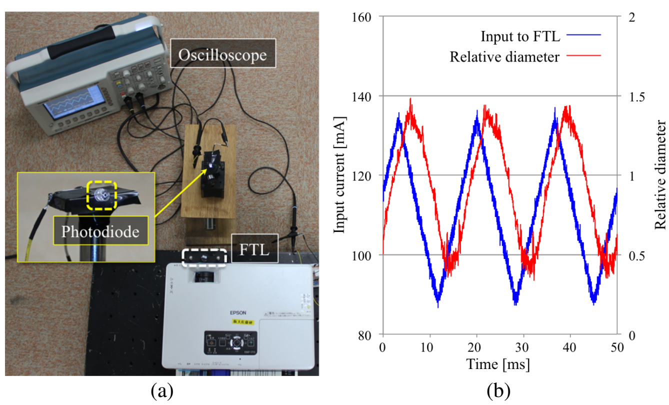

Fig. 5. Linearity verification: (a) measurement system; (b) measured data.

4.3 Image Quality Evaluation

We evaluated the projected image quality produced by the proposed focal sweep projection. We compared projected results from the proposed method with those obtained with normal projection (i.e., fixed focal length and original images without blur compensation). Three types of experiments were conducted with different surfaces; i.e., two surfaces with different depths (Fig. 1), a tilted surface (Fig. 7), and a moving surface (Fig. 8). In addition to these experiments using static images, we conducted another experiment using a moving image.

Two planar surfaces were placed at different depths (200 and 400 mm) from the FTL. A parrot image was used for the experiment (Fig. 1). The original image was compensated for the IPSFs to generate a projection image for focal sweep projection. Normal projection was performed with three different focusing distances, i.e., 200, 300, and 400 mm. Figure 1 shows four projected results, one obtained by focal sweep projection, and the remaining three obtained by normal projection. Focal sweep projection provided a focused image on both surfaces. In contrast, normal projection produced images that were either focused on only one surface (focusing distance, 200 and 400 mm) or were out-of-focus on both surfaces (focusing distance, 300 mm).

Table 1. SSIM evaluation results for images shown in Fig. 7.

Image	Focal sweep projection	Normal projection
Lenna	**0.60**	0.52
Town	**0.45**	0.39
Mountain	**0.53**	0.50

In the tilted surface experiment, the surface was placed so that the left edge of the projected image was displayed at a depth of 200 mm from the FTL, and the right edge was at 400 mm (Fig. 7, top-left). We fixed the focusing distance at 400 mm from the FTL for a normal projection. Three different natural images were used as original images (Fig. 7, bottom-left). Projected results captured and rectified for comparison are shown on the right side of Fig. 7. As can be seen, the left parts of the projected results of normal projection are blurred and lose the high spatial frequency components of the original images, while focal sweep projection provides a nearly all-in-focus image. We quantitatively evaluated image quality using the structural similarity index (SSIM), which is a method for assessing the perceptual quality of a distorted image, compared to the original [23]. From the results shown in Table 1, we can confirm that the proposed focal sweep projection method provided the best image quality.

In the moving surface experiment, we freely moved a flat surface by hand within sweep range (i.e., between 200 and 400 mm from the FTL), as shown in Fig. 8, which shows the results of focal sweep projection and normal projection. Note that we fixed the focusing distance at 300 mm for normal projection. We confirmed that focal sweep projection always provided a focused image, while normal projection only focused the image at approximately 300 mm from the FTL. Refer to the supplementary video to see the entire experimental sequence.

We conducted another experiment using a moving image [4] with a curved surface (Fig. 9). We fixed the focusing distance at 400 mm from the FTL for a normal projection. Exact synchronization of the FTL and the projector is typically required for displaying moving images without temporal artifacts. Thanks to the periodical nature of the FTL's modulation, the phase synchronization is not required as long as the frequency of the modulation is equal to the integral multiple of the projector's refresh rate. In this experiment, we set the refresh rate of the projector as 60 Hz. Projected results were captured with a video

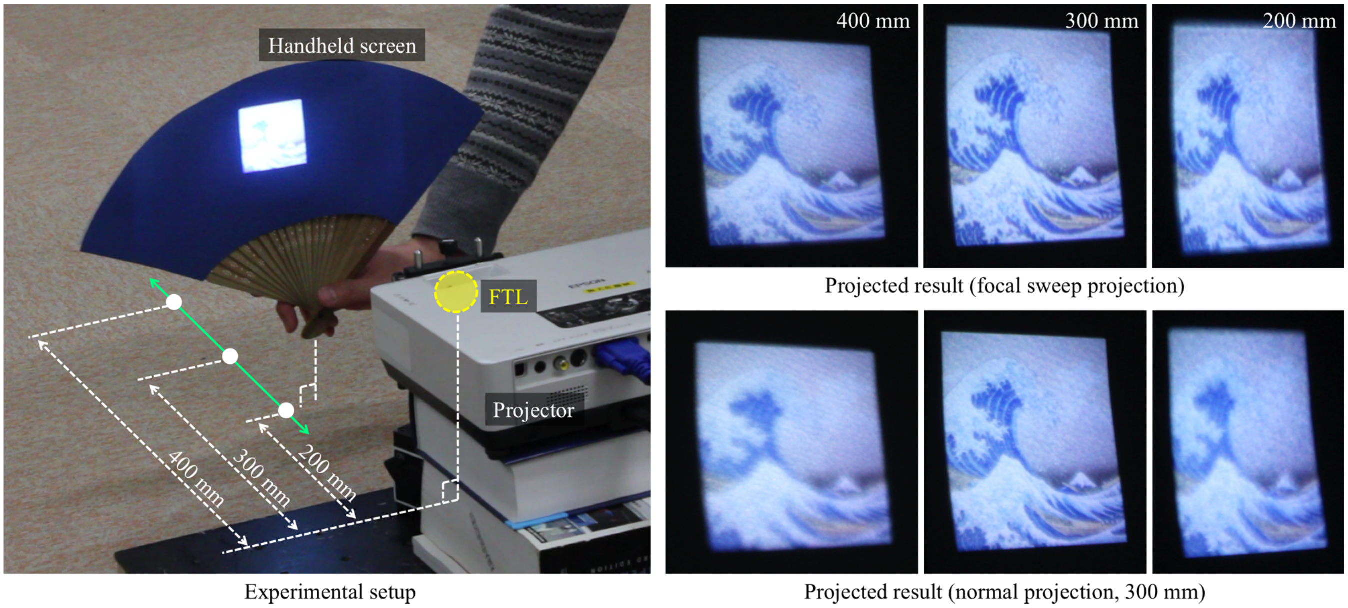

Fig. 8. Projection on the moving handheld screen: (left) experimental setup (green arrow indicates the moving range of the screen); (right) projected results at different depths.

camera. Three frames are picked up from the captured sequence and shown on the right side of Fig. 9 (see supplementary video for the entire sequence). From the results, we confirmed that the proposed focal sweep projection method provided better-focused images than normal projection.

4.4 Evaluation of Shape Measurement Accuracy

Besides the enhancement of projected image quality, an extended DOF projector using the proposed focal sweep technique also enhances the accuracy of shape measurement for active stereo methods using ProCams when measuring an object with large depth variance. Essentially, structured light patterns are projected on the object, and reflections are captured to acquire pixel correspondences between the camera and the projector, which are then used in shape computation through triangulation [21]. Shape data measured by ProCams are widely used in current VR/AR applications.

ProCams-based shape measurement suffers from the narrow DOF of standard projectors. The entire volume of the object must be within the DOF. Once a part of the object surface is located outside of DOF, the projected structured light patterns become blurred. Consequently, pixel correspondences cannot be acquired accurately. Through an experiment, we verified how the proposed focal sweep technique improves shape measurement accuracy for an object with large depth variance.

We applied a gray code pattern projection technique [22] that is widely applied in many fields. The pattern consisted of nine binary fringe patterns ($= 2^9 > 300$ pixels) for both horizontal and vertical directions. For robust pattern extraction from captured images, we applied Manchester coding to the pattern. In particular, in addition to the original fringe patterns, the inverted patterns were projected, and both patterns were captured. We then subtracted the captured inverted pattern from the corresponding original pattern. Consequently, the positive pixels in the subtracted image represented the binary code of the projected original fringe pattern.

We measured the shape of the tilted surface used in the previous experiment (Section 4.3). Shape measurement was performed using the focal sweep projection and normal projection. For normal projection, we fixed the focusing distance at 400 mm from the FTL. The measured shapes are shown at the bottom-left of Fig. 10; i.e., two-dimensional slices of the measured shapes (dashed blue line at the top-left of the figure). From the results, we see that the error was smaller with focal sweep projection than normal projection. Specifically, the shape data became noisy where projected patterns were blurred using normal projection. To evaluate the error quantitatively, we fitted a plane independently to each measured shape using a least squares method, and calculated the mean difference from the measured points to the plane. The mean difference was 0.21 mm in the focal sweep projection and 0.26 mm in the normal projection. Thus, we confirmed that focal sweep projection provided better measurement results with fewer errors than normal projection.

We analyzed these results in details. We compared the captured images of the projected finest patterns (vertical fringe, one pixel wide), as well as the extracted codes between the two projections. As shown in the right of Fig. 10, for normal projection, the captured pattern was not clear. Consequently, approximately one third of the fringes were not extracted correctly. On the other hand, we can see clearer fringes in the captured pattern, and sharp fringes were extracted successfully using focal sweep projection.

5 Discussion

We have shown that the image quality of the projected results obtained using the proposed fast focal sweep projection is superior to normal projection. We have also shown that focal sweep projection can measure the shape of an object with large depth variance more accurately than normal projection. Implementing the extended DOF projector with our approach is easy, quick, and cost efficient. One can extend the DOF of their own projector by simply placing an FTL before the projector, which does not typically require disassembling the unit. Therefore, we believe that the proposed approach has a potential for application in various existing projection systems, and can lead to new applications wherein projection has not been considered a suitable display technology due to the defocus issue.

The proposed method shares a limitation with other extended DOF projector methods (single-projector approach; Section 2.1) that apply blur compensation techniques to correct the original images before projection. In general, due to the limited dynamic range of projectors, projection images, to which a blur compensation technique is applied, loose some contrast compared to a normal projection. More technically, blur compensation techniques suffer a trade-off between ringing artifacts and contrast degradation [11]. Given a fixed PSF or IPSF, one cannot simultaneously increase the contrast of a projected result and decrease ringing artifacts. These issues can be improved

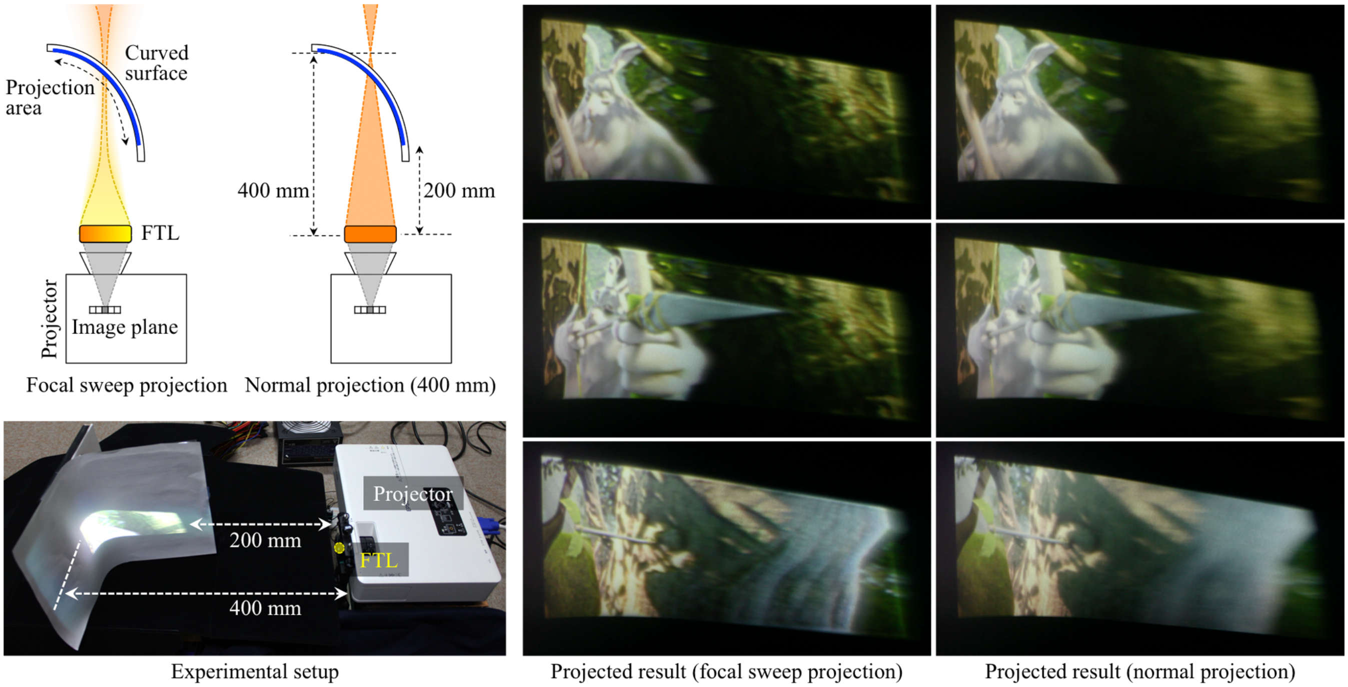

Fig. 9. Extended DOF projector demonstration using a moving image [4] with a curved projection surface: (top-left) comparison of proposed focal sweep projection and normal projection (fixed focusing distance, 400 mm); (bottom-left) experimental setup; (right) projected results of different frames.

with better PSFs, whose Fourier transform do not take zero nor nearly equal to it over the entire frequency band. By combining the proposed method with a real-time range sensor, such as the Kinect [16], sweep range can be optimized adaptively to allow the complete coverage of a projection target while minimizing sweep distance. Shorter sweep distance results in an IPSF that is closer to an impulse function comprising non-zero equal portions of all possible frequencies. Therefore, sweep range optimization can potentially achieve better image quality than naïve fixed sweep ranges.

The proposed method has other limitations due to the limited capabilities of the currently applied FTL. First, as described in Section 4.1, we could only use a part of the projection image (i.e., the center 300×300 region) due to the vignetting effect of the FTL. Second, focal sweep technology is not suitable for sequential color projectors, such as DLP (digital light processing). Such projectors display red, green, and blue channels at different time periods, i.e., the refresh rate of color channels is 180 Hz for a standard 60 Hz projector. Therefore, none of the color channels sweep for the entire sweep range with a periodical focal modulation at 60 Hz. These implementation problems can be solved in the future once an upgraded FTL with sufficiently large aperture and the ability to modulate focal length at 180 Hz and higher is developed.

In the experiment using moving images (Section 4.3), the projection image generation including the blur compensation took around fifty minutes for each frame with a computer (CPU: Intel Xeon E5606 2.13 GHz, RAM: 24 GB) and our current non-optimized implementation. This process can be much further optimized using GPU, as a previous work demonstrated real-time blur compensation [9].

6 Conclusion

We have introduced the concept and the first implementation of an extended DOF projector based on a fast focal sweep technique. We have proposed a simple approach, i.e., fast focal length modulation is achieved by placing an FTL before a projector's objective. The proposed method is an open-loop process that requires only a single offline IPSF calibration, while other conventional methods for extending projector DOF require online PSF measurement whenever a projection target or a projector moves. We have shown the computational model of projected IPSFs and numerically demonstrated the IPSF's approximate invariance to scene depths, which was confirmed experimentally using a prototype system. We performed projection experiments with three different projection surfaces, including a moving surface. The results show that the proposed method always provides better image quality than normal projection techniques with fixed focusing distances. We also demonstrated that a structured light pattern projection technique with the proposed method can measure the shape of an object with large depth variance more accurately than normal projection techniques.

In future, we will work on sweep range optimization to allow adaptive adjustment depending on the shape and distance to a projection surface to realize a further extended DOF projector.

Acknowledgments

This work was supported by a Grant-in-Aid for Scientific Research on Innovative Areas "Shitsukan" (No. 22135003) from MEXT, Japan.

References

[1] AAXA Technologies Inc., 2014. `http://www.aaxatech.com/`.

[2] D. Bandyopadhyay, R. Raskar, and H. Fuchs. Dynamic Shader Lamps: Painting on Movable Objects. In *Proceedings of IEEE/ACM International Symposium on Augmented Reality (ISAR)*, pages 207–216, 2001.

[3] A. Bermano, P. Brüschweiler, A. Grundhöfer, D. Iwai, B. Bickel, and M. Gross. Augmenting Physical Avatars Using Projector Based Illumination. *ACM Transactions on Graphics*, 32(6):189:1–189:10, 2013.

[4] Big Buck Bunny., 2014. `https://peach.blender.org/`.

[5] O. Bimber and A. Emmerling. Multifocal Projection: A Multiprojector Technique for Increasing Focal Depth. *IEEE Transactions on Visualization and Computer Graphics*, 12(4):658–667, 2006.

[6] O. Bimber, D. Iwai, G. Wetzstein, and A. Grundhöfer. The Visual Computing of Projector-Camera Systems. *Computer Graphics Forum*, 27(8):2219–2254, 2008.

[7] O. Bimber and R. Raskar. *Spatial Augmented Reality: Merging Real and Virtual Worlds*. A. K. Peters Ltd., 2005.

[8] M. S. Brown, P. Song, and T.-J. Cham. Image Pre-Conditioning for Out-of-Focus Projector Blur. In *Proceedings of IEEE Conference on Computer Vision and Pattern Recognition (CVPR)*, volume II, pages 1956–1963, 2006.

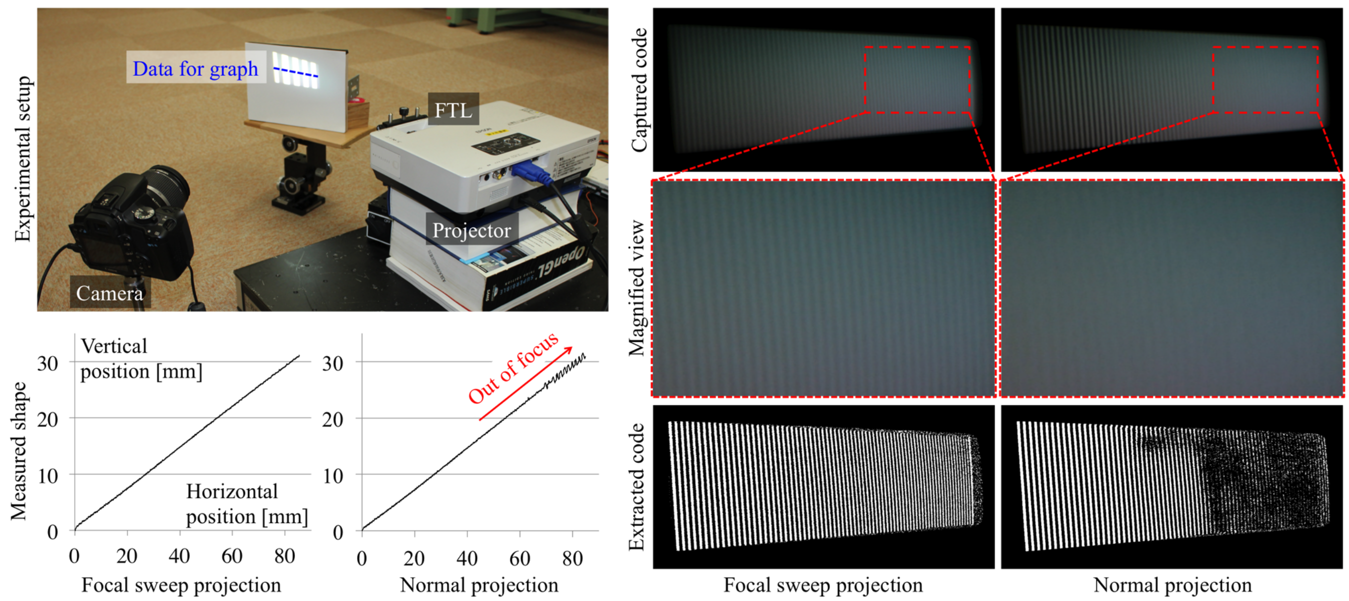

Fig. 10. Shape measurement experiment: (top-left) experimental setup; (bottom-left) two-dimensional slices of measured shapes on the dashed blue line in the top-left figure (horizontal and vertical directions for graphs are defined in an arbitrarily assigned world coordinate system independent of camera and projector coordinate systems); (top-right, middle-right) raw images used to capture the finest gray code pattern (vertical fringe pattern of one pixel width projected on a tilted surface); (bottom-right) extracted code patterns.

[9] M. Grosse, G. Wetzstein, A. Grundhoefer, and O. Bimber. Coded Aperture Projection. *ACM Transactions on Graphics*, 29(3):22:1–22:12, 2010.

[10] G. Häusler. A Method to Increase the Depth of Focus by Two Step Image Processing. *Optics Communications*, 6(1):38–42, 1972.

[11] Y. Ji, J. Ye, S. B. Kang, and J. Yu. Image Pre-compensation: Balancing Contrast and Ringing. In *Proceedings of IEEE Conference on Computer Vision and Pattern Recognition (CVPR)*, 2014.

[12] M. Kalloniatis and C. Luu. Temporal resolution. In H. Kolb, R. Nelson, E. Fernandez, and B. Jones, editors, *Webvision – The Organization of the Retina and Visual System*. 2014. `http://webvision.umh.es/webvision/temporal.html`.

[13] S. Kuthirummal, H. Nagahara, C. Zhou, and S. K. Nayar. Flexible Depth of Field Photography. *IEEE Transactions on Pattern Analysis and Machine Intelligence*, 33(1):58–71, 2011.

[14] S. Liu and H. Hua. Extended Depth-of-Field Microscopic Imaging with a Variable Focus Microscope Objective. *Optics Express*, 19(1):353–362, 2011.

[15] D. Miau, O. Cossairt, and S. K. Nayar. Focal Sweep Videography with Deformable Optics. In *Proceedings of IEEE International Conference on Computational Photography (ICCP)*, pages 1–8, 2013.

[16] Microsoft Corporation., 2014. `http://www.xbox.com/kinect/`.

[17] M. Minsky. Microscopy Apparatus, 1961. US Patent 3013467.

[18] H. Nagahara, S. Kuthirummal, C. Zhou, and S. K. Nayar. Flexible Depth of Field Photography. In *Proceedings of European Conference on Computer Vision (ECCV)*, pages 60–73, 2008.

[19] M. Nagase, D. Iwai, and K. Sato. Dynamic Defocus and Occlusion Compensation of Projected Imagery by Model-Based Optimal Projector Selection in Multi-projection Environment. *Virtual Reality*, 15(2):119–132, 2011.

[20] Optotune AG., 2014. `http://www.optotune.com/`.

[21] J. Salvi, J. Pages, and J. Batlle. Pattern codification strategies in structured light systems. *Pattern Recognition*, 37(4):827–849, 2004.

[22] K. Sato and S. Inokuchi. Range-Imaging System Utilizing Nematic Liquid Crystal Mask. In *Proceedings of IEEE International Conference on Computer Vision (ICCV)*, pages 657–661, 1987.

[23] Z. Wang, A. C. Bovik, H. R. Sheikh, and E. P. Simoncelli. Image Quality Assessment: From Error Visibility to Structural Similarity. *IEEE Transactions on Image Processing*, 13(4):600–612, 2004.

[24] Waterloo Maple Inc., 2014. `http://www.maplesoft.com/`.

[25] L. Zhang and S. Nayar. Projection Defocus Analysis for Scene Capture and Image Display. *ACM Transactions on Graphics*, 25(3):907–915, 2006.